J Solid State Electrochem (2013) 17:1775–1783
DOI 10.1007/s10008-012-1737-0

ORIGINAL PAPER

Ionic conductivity enhancement in the solid polymer electrolyte PEO_9LiTf by nanosilica filler from rice husk ash

M. A. K. L. Dissanayake · W. N. S. Rupasinghe ·
J. M. N. I. Jayasundara · P. Ekanayake ·
T. M. W. J. Bandara · S. N. Thalawala ·
V. A. Seneviratne

Received: 17 August 2011 / Revised: 25 March 2012 / Accepted: 27 March 2012 / Published online: 29 April 2012

Abstract Rice husk ash is a cheap raw material available in abundance in rice-growing countries. It contains around 85–90 % amorphous silica. Rice husk ash, when subjected to a simple chemical precipitation method, will produce nanosilica which can be used for many industrial and technological applications. In this work, we have successfully synthesized nano-sized silica from local rice husk ash and prepared the nanocomposite solid polymer electrolyte, $PEO_9LiTf:SiO_2$. The resulting electrolyte has been characterized by X-ray diffraction, differential scanning calorimetry, atomic force microscopy, Fourier transform infrared spectroscopy, and complex impedance spectroscopy. The electrolyte shows about a 12-fold increase in ionic conductivity at room temperature due to the silica filler. In the nanocomposite electrolyte, nanosilica particles obtained from rice husk ash behaved very similarly to the commercial grade nanosilica and had a size distribution in the 25- to 40-nm range. As already suggested by us and by others, the O^{2-} and OH^- surface groups in the filler surface interact with the Li^+ ions and provide hopping sites for migrating Li^+ ions through transient H bonding, creating additional high-conducting pathways. This would contribute to a substantial conductivity enhancement through increased ionic mobility. An additional contribution to conductivity enhancement, particularly at temperatures below 60 °C, appears to come from the increased fraction of the amorphous phase, as evidenced from the reduced crystallite melting temperature and the reduced enthalpy of melting due to the presence of the filler.

Keywords Rice husk ash · Nanosilica · PEO:LiTf electrolyte · Conductivity enhancement

Introduction

Nanosilica from rice husk ash

Rice husks or rice hulls are the outer cover of the rice grains in a rice plant. To provide natural protection to the rice seed during the growing period, the husk is made of hard materials, including opaline silica and lignin. The husk is indigestible to humans. During the rice milling process, the husks are removed from the grain to create brown rice, which is then milled further to remove the bran layer, producing white rice. Rice husks are an inexpensive by-product of rice milling and are available in abundance in most rice-producing countries.

A number of rice-producing countries including India, Thailand, and China are currently conducting research on many possible industrial uses of rice husk. During the milling of paddy, about 78 % of weight is received as rice, broken rice, and bran. The remaining 22 % of the weight of paddy is received as husk. For every 1,000 kg of paddy milled, about 220 kg (22 %) of husk is produced, and when this husk is burnt in the boilers, about 55 kg (25 %) of rice

---

Electronic supplementary material The online version of this article (doi:10.1007/s10008-012-1737-0) contains supplementary material, which is available to authorized users.

M. A. K. L. Dissanayake · W. N. S. Rupasinghe ·
J. M. N. I. Jayasundara · P. Ekanayake · S. N. Thalawala ·
V. A. Seneviratne
Department of Physics, University of Peradeniya,
Peradeniya, Sri Lanka

M. A. K. L. Dissanayake (✉) · W. N. S. Rupasinghe
Institute of Fundamental Studies,
Kandy, Sri Lanka
e-mail: makldis@yahoo.com

T. M. W. J. Bandara
Department of Physical Sciences, University of Rajarata,
Mihintale, Sri Lanka

husk ash (RHA) is generated. About 20 million tons of RHA is produced annually worldwide. This RHA is a great environment threat causing damage to the land and the surrounding area in which it is dumped. Lots of ways are being thought of for disposal by making commercial use of this RHA.

Rice husk contains about 75 % organic volatile matter, and the remaining 25 % of the weight of this husk is converted into ash when rice husk is burnt. This RHA in turn contains around 85–90 % amorphous silica. RHA, when subjected to a simple precipitation method, will produce nanosilica. The precipitation can be done, for example, by refluxing RHA silica in boiling NaOH. Thus, we have a simple chemical method which can be performed in any chemistry laboratory to obtain nanosilica from rice husk ash, which is a very cheap raw material available in abundance in rice-growing countries.

The use of nanosilica from RHA in nanocomposite PEO-based polymer electrolytes

Solid polymer electrolytes are emerging as a class of technologically important novel materials for various applications such as high energy density lithium ion rechargeable batteries, fuel cells, supercapacitors, photoelectrochemical solar cells, electrochromic displays, and smart windows. Among these, poly(ethylene oxide) (PEO)-based polymer electrolytes appear to be among the best candidates to be used as polymer electrolyte membranes because of their solvation power, complexion ability, and ion transport mechanism directly connected with the alkaline salt (Li^+). However, the ionic conductivity of PEO:LiX (X=ClO_4^-, $CF_3SO_3^-$, BF_4^-, PF_6^-, etc.) electrolytes at ambient temperature are in the 10^{-7}- to 10^{-6}-S cm^{-1} range, not high enough for most practical applications. In order to enhance the ionic conductivity of PEO-based polymer electrolytes, various strategies have been employed [1, 2]. Ionic conductivity enhancement in these polymer electrolytes have been achieved mainly by using two techniques [3, 4]. One is the dispersion of nano-sized inorganic ceramic filler particles such as Al_2O_3, SiO_2, and TiO_2 in the polymer electrolyte to produce nanocomposite solid polymer electrolytes [3–9]. The other technique is the incorporation of low-molecular-weight plasticizers such as ethylene carbonate, propylene carbonate, and polyethylene glycol into the conventional PEO–LiX systems to produce plasticized polymer electrolytes [7, 10, 11]. Plasticization is the conventional way to reduce the crystallinity and increase the amorphous phase content of the polymer electrolytes. However, conductivity enhancement in plasticized polymer electrolytes is achieved at the expense of their mechanical strength [8, 9]. The addition of nano-sized ceramic fillers, on the other hand, would lead to an enhancement in conductivity while retaining the mechanical strength of the polymer electrolyte membrane. This paper reports the result of a study on the electrical conductivity enhancement of a PEO-based polymer electrolyte prepared by incorporating nano-sized silica obtained from rice husk ash. The resulting PEO_9-LiTf+10 wt% SiO_2 nanocomposite polymer electrolyte has been characterized by X-ray powder diffraction (XRD), Fourier transform infrared spectroscopy (FTIR), atomic force microscopy (AFM), differential scanning calorimetry (DSC), DC polarization tests, and ionic conductivity. The best nanocomposite electrolyte has shown about a 12-fold increase in lithium ion conductivity at room temperature due to the incorporation of the silica filler. As far as we are aware, this is the first report of using nano-sized silica powder synthesized from rice husk ash for ionic conductivity enhancement in a polymer electrolyte.

Experimental

Preparation of nanosilica from rice husk ash

Pure silica powder was obtained from RHA using the method reported by Thuadaij et al. [12]. RHA was washed with distilled water and burnt at 700 °C for 6 h. Of the RHA sample, 10 g was stirred in 80 ml of 3.0 N NaOH solution and boiled in a covered Erlenmeyer flask for 3 h. The solution was filtered and the residue washed with 20 ml of boiling water. The filtrate was allowed to cool down to room temperature; 5 N H_2SO_4 was added until the pH reaches 2 and then NH_4OH added until the pH reaches 8.5. Then, the filtrate was kept at room temperature for 3.5 h and subsequently dried at 120 °C for 12 h (Fig. 1a, b).

Reactions:

$$\begin{aligned} SiO_2 + 2NaOH &\rightleftarrows Na_2SiO_3 + H_2O \\ Na_2SiO_3 + H_2SO_4 &\rightleftarrows SiO_2 + Na_2SO_4 + H_2O \end{aligned}$$

It is interesting to note that 18 g of RHA gives about 11 g of pure silica, yielding a 65 % conversion.

Pure silica obtained from RHA was refluxed with 6 N HCl for 4 h and washed repeatedly using distilled water. It was then dissolved in 2.5 N NaOH by continuous stirring for 10 h. After that, conc. H_2SO_4 was added to adjust pH in the range of 7.5–8.5. The precipitated silica was washed repeatedly with warm distilled water until the filtrate became completely alkali-free and dried at 50 °C for 48 h in the oven to obtain nanosilica powder (Fig. 1c).

Preparation of polymer electrolyte films

PEO (MW=4×10^6), SiO_2 (size, 10–20 nm; specific surface area, 390 m^2 g^{-1}), and lithium trifluoromethanesulphonate ($LiCF_3SO_3$), commonly known as lithium triflate (LiTf, purchased from Aldrich), were used as starting materials along with RHA nano silica. Prior to use, PEO, LiTf, and SiO_2 were vacuum-dried for 24 h at 50, 120, and 200 °C, respectively. PEO (0.5 g) and LiTf (0.197 g) were dissolved

Fig. 1 Photographs of rice husk ash burnt to 700 °C (**a**), prepared pure silica (**b**), and prepared nanosilica (**c**)

in acetonitrile so that the oxygen-to-lithium ion ratio is 9:1. The above mixture was stirred for 24 h at room temperature, the slurry was cast on a Teflon support, and the solvent was allowed to evaporate. The resulting polymer electrolyte film was vacuum-dried at room temperature for 24 h. Nanocomposite polymer electrolyte samples were also prepared using the aforementioned procedure by adding 10 wt% nano-SiO_2 filler obtained from rice husk ash (or commercially purchased) for the total weight of PEO+LiTf electrolyte.

Characterization of nanosilica

The phases of the RHA nanosilica obtained from RHA and also commercially purchased nanosilica were determined using powder X-ray diffraction. The major chemical groups present in nanosilica from RHA were identified by FTIR spectroscopy using Thermo Scientific Nicolet 6700 FTIR spectrometer in the transmission mode with a resolution of 4 cm^{-1}. The particle size and morphology were examined using Veeco Caliber SPM/AFM. With the assumption of spherical shape, the size of the particles was determined from the number-averaged particle diameter. For this, a nanosilica sample (1 mg) was sonicated for 2 h in acetone (20 ml) and a small amount of silica suspension taken using a dropper and spread on a thin glass slide of 1-cm^2 size. The glass slide was then scanned in the tapping mode. All the above characterization methods were repeated using commercially available silica as well, and the results were compared with the results obtained for the nanosilica synthesized from RHA. For thermal analysis, measurements were taken using a Mettler Toledo differential scanning calorimeter covering a temperature range from −120 to +120 °C at a heating/cooling rate of 10 °C min^{-1}.

Electrical characterization of composite solid polymer electrolyte films

Wagner's DC polarization method

For a solid electrolyte to be used as a separator in electrochemical devices, such as rechargeable batteries, fuel cells, super capacitors, etc., the electronic conductivity must be negligibly small compared to the ionic conductivity in order to minimize internal short circuiting and to achieve higher power densities. Due to its simplicity, the most widely used technique to estimate the ionic and electronic contributions to the total conductivity in a solid electrolyte has been the Wagner DC polarization method [13].

We have used Wagner's DC polarization technique where the electrolyte sample was sandwiched between two ion blocking electrodes and a constant DC potential of 2 V was applied across the sample by a potentiostat; the resulting current was monitored by a sensitive digital multimeter as a function of time. Under the influence of the DC field, cations migrate to the negative electrode and anions to the positive electrode, thus polarizing the material. When the back potential created by the concentration gradient exactly opposes the applied potential, the ions no longer carry current and the cell is completely polarized. Thus, any resulting steady-state current is only due to electronic contribution. Just after switching on the circuit, the initial total current, I_t, started to quickly decrease with time, corresponding to the polarization of ionic species in the electrolyte, and becomes constant in the fully polarized situation. At this steady stage, the residual current is only electronic current (I_e). We have used the DC polarization measurements to establish that the material is predominantly an ionic conductor and not to calculate the ionic and electronic transport numbers. This is because, experimentally, the actual value of the initial total current (at time t=0) is difficult to measure accurately. This is an inherent limitation of this method. Also, for a measurement with reasonable accuracy, the electrode overpotential, which is the potential drop at the

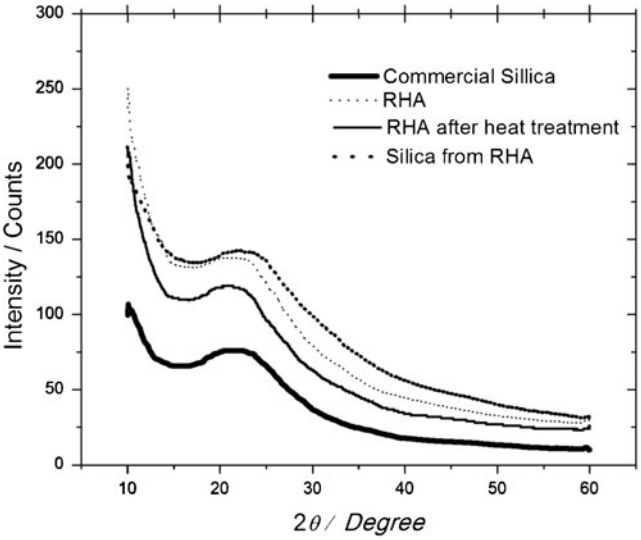

Fig. 2 X-ray diffractograms of synthesized nanosilica and commercially available silica

two blocking electrodes, should be taken into account, unless they are negligibly small. If one is interested in actually determining the ionic and electronic transport numbers accurately, a better method would be to use a four-probe technique instead of the usual two-electrode method [14].

Impedance measurements

The ionic conductivity of the polymer electrolyte samples was determined by the AC complex impedance method with a computer-controlled Solatron SI-1260 impedance analyzer in the frequency range 20 Hz–10 MHz. Disc-shaped thin films sandwiched between two stainless steel electrodes were used for impedance measurements. The temperature of the sample was varied from 30 to 80 °C at approximately 5 °C intervals. The temperature of the sample was allowed to stabilize at each measuring temperature for about 30 min. The ionic conductivity at each temperature was extracted from the impedance data.

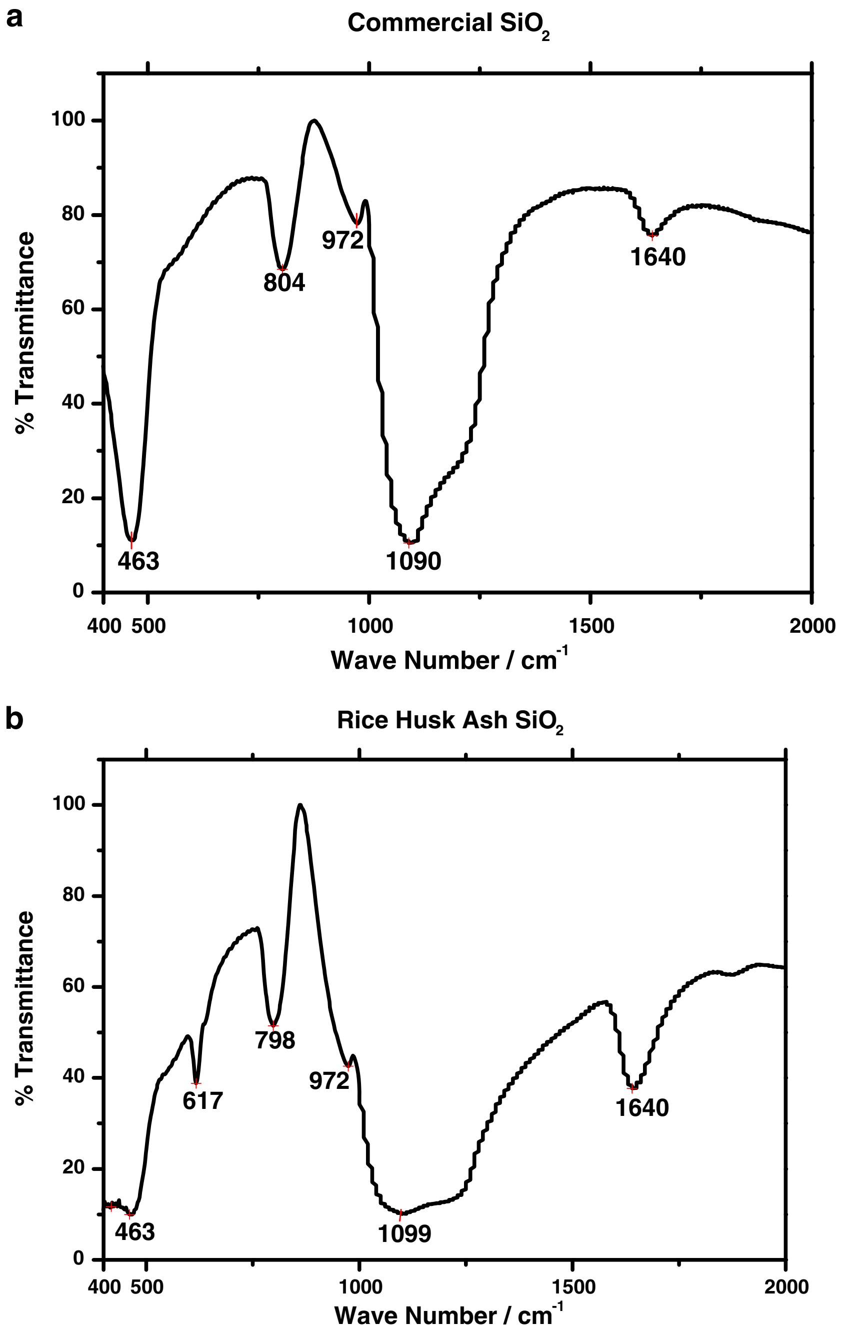

Fig. 3 FTIR spectra of commercially available nanosilica (**a**) and nanosilica synthesized from rice husk ash (**b**)

Table 1 Assignment of FTIR peak positions to possible vibration modes of commercially available nanosilica and nanosilica produced from RHA

Mode	Wavenumber (cm^{-1})	
	Commercial SiO_2	RHA SiO_2
Si–O bending	463	463
Cristobalite	–	617
Si–O out-of-plane deformation	804	798
Si–OH stretching modes	972	972
Si–O–Si stretching	1,090	1,099
C–O stretching	1,640	1,640

Results and discussion

The XRD diffractogram of nanosilica synthesized from RHA shows a strong broad peak between 21° and 25° (2*θ*), suggesting that the silica powder is in the amorphous phase. The XRD diffractograms of RHA and rice husk ash burnt at 700 °C show similar strong broad peaks between 21° and 25° (Fig. 2).

The FTIR spectra of commercial grade nanosilica and RHA nanosilica are shown in Fig. 3a, b. Both spectra show similar features, confirming that what we have obtained from RHA is pure nanosilica. Some major chemical groups present in silica can be identified in these spectra. These peak assignments are shown in Table 1. Here, we refer to the band positions of the RHA silica spectrum.

The characteristic bands at 1,099, 798, and 463 cm^{-1} correspond to the Si–O–Si stretching, bending, and out-of-plane deformation of Si–O bonds, respectively. The corresponding positions for the commercial nanosilica are at 1,090, 804, and 463 cm^{-1}, respectively. The peak at 1,640 cm^{-1} seen in the spectra of both samples can be attributed to the C–O stretching of carbon impurity atoms in the sample.

The above observations agree well with the FTIR spectra of silicon dioxide thin films deposited by metal organic-based plasma-enhanced chemical vapor deposition by Shokri et al. [15], for nanosilica prepared using the sol–gel method by Waseem et al. [16], and for amorphous silica prepared from oil shale residue by Xu et al. [17]. The weak band appearing at 617 cm^{-1} for the RHA nanosilca is characteristic of the crystalline cristobalite which may be present as a trace impurity originated during the burning of rice husk [18]. The mineral cristobalite is a high-temperature polymorph of silica having the same chemical formula, SiO_2, but a distinct crystal structure. The very weak absorption band at 972 cm^{-1} seen for both nanosilica samples can be attributed to the Si–OH stretching modes of surface silanol, as seen by other groups as well [16, 19, 20].

According to the AFM images shown in Fig. 4, the nanosilica particles obtained from rice husk ash exist in agglomerate form. These silica particles do not possess a uniform particle size, but had size distribution in the 25- to 40-nm range.

DSC thermograms obtained during the second heating run for the electrolyte samples containing 10 % SiO_2 (RHA) and 10 % SiO_2 (Comm) are compared in Fig. 5. The weights of the electrolyte samples with commercial silica filler and RHA silica filler are 9.4 and 19.3 mg, respectively. Measurements were taken during the second heating run in order to eliminate the negative effects due to the thermal history of the sample.

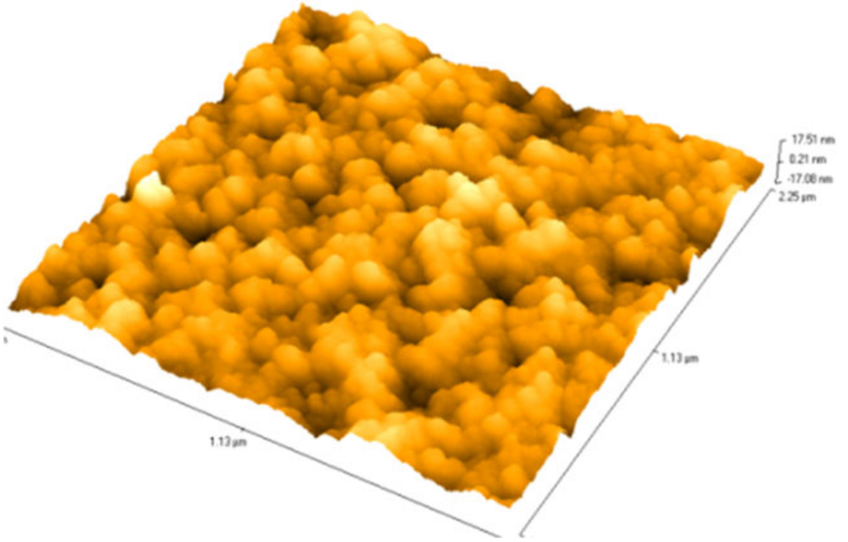

Fig. 4 Atomic force microscopy photograph of nanosilica grains obtained from rice husk ash exhibiting grain size and grain distribution. Area shown in the picture correspond to 2.25 micron × 2.25 micron

Fig. 5 DSC thermograms of the polymer electrolyte samples $PEO_9LiTf+10$ wt% SiO_2 with the commercial nanosilica filler and with the RHA nanosilica filler

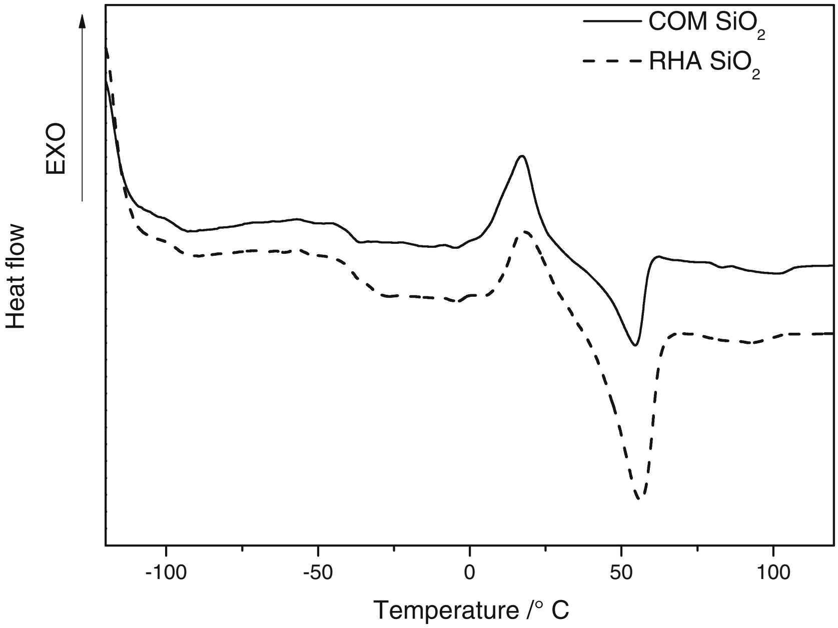

The two traces and the positions of thermal transitions are essentially the same for both samples, indicating that the nanosilica obtained from rice husk has the same thermal behavior as the commercial nanosilica. We have performed the DSC scans mainly as a comparative test to compare the thermal behavior of the polymer electrolyte with RHA nanosilica and with commercial nanosilica. Both samples show a crystallization peak, followed by a melt peak, as expected. The crystallization peak around 20 °C is very likely due to the delayed crystallization of the material.

The glass transition temperatures (T_g) and the melting temperatures (T_m) of $PEO_9LiTf+10$ wt% SiO_2 (RHA) electrolyte, determined using DSC measurements, are −43.5 and 56.5 °C, respectively. The T_g of filler-free electrolyte is −44 °C, according to this work (curve not shown) as well as our previous work [31]. Although the T_g remains essentially unchanged compared with the filler-free sample, the PEO crystallite melting temperature, T_m, has been reduced by about 5 °C due to the filler, suggesting that the PEO crystallite size has reduced due to the presence of the SiO_2

Fig. 6 DC polarization test results: variation of current through the sample with time for the polymer electrolyte $PEO_9LiTf+10$ wt% SiO_2 (RHA)

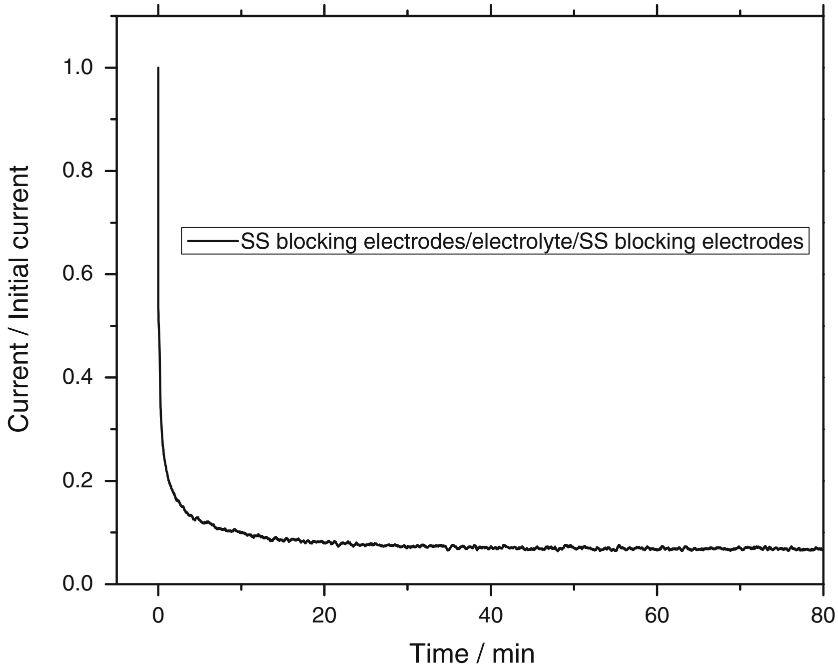

filler. According to our previous work on $PEO_9LiTf+10$ % (wt) Al_2O_3 system, T_m has reduced from 58 to 54 °C due to the addition of 10 wt% nano-Al_2O_3 filler [31]. The results for the nanosilica-added system appear to follow the same behavior. We infer from the drop in the value of the PEO crystallite melting temperature, T_m by about 5 °C, that the crystallite size has diminished, suggesting an increase in the fraction of the amorphous phase in the filler-added composite material.

The values of the melting enthalpy change of the filler-added samples, calculated from the area under the melting peak of the corresponding DSC isotherm and normalized to the weight of PEO in the sample, are $\Delta H_m(\text{comm})=52.1\ \text{Jg}^{-1}$ and $\Delta H_m(\text{RHA})=50.6\ \text{Jg}^{-1}$ for the commercial silica-added sample and RHA silica-added sample, respectively. As the reference ΔH_m (neat PEO), we will use the melting enthalpy for 100 % crystalline PEO as 213.7 Jg^{-1}, taken from [22, 23]. We can therefore calculate the relative percentages of crystallinity in each sample as follows:

$$\begin{aligned} X_c(\text{comm}) &= [\Delta H_m(\text{comm})/\Delta H_m(\text{neat PEO})] \times 100 \\ &= \left[52.1\text{Jg}^{-1}/213.7\text{Jg}^{-1}\right] \times 100 = 24.4\% \\ X_c(\text{RHA}) &= [\Delta H_m(\text{RHA})/\Delta H_m(\text{neat PEO})] \times 100 \\ &= \left[50.6\text{Jg}^{-1}/213.7\text{Jg}^{-1}\right] \times 100 = 23.7\% \end{aligned}$$

The crystallinity of neat PEO, according to [20], is 84.87 %. According to the above result, the crystallinity has reduced considerably due to the incorporation of the salt LiTf as well as the silica filler. The percentages of crystallinity in the two filler-added samples are comparable, providing further evidence to the similarity in their behavior in the nanocomposite electrolyte. Reductions of the crystallite melting temperature, T_m, and the crystallinity, X_c, both suggest that the interaction between the polymer and the filler has caused a reduction in the crystallite size of the polymer, thereby increasing the fraction of the amorphous phase content.

From the DC polarization test results of the nanocomposite polymer electrolyte with RHA nanosilica, it was observed that the current through the DC voltage-based sample rapidly decays with time and goes to a very low steady value after about 80 min (Fig. 5). Under the influence of the DC field, cations migrate to the negative electrode and anions to the positive electrode. As the cell polarizes, charge carriers blocked at inner dielectric boundary layers (on the mesoscopic scale) or external electrodes (on a macroscopic scale) lead to a separation of charges. When the back potential created by the concentration gradient exactly opposes the applied potential, the ions no longer carry current and the cell is completely polarized with respect to the ionic species. Thus, any resulting steady-state current is only due to the electronic contribution. The shape of the current vs. time curve suggests that conductivity is predominantly due to the ions in the polymer electrolyte (Fig. 6).

Variation of ionic conductivity with inverse temperature from 30 to 80 °C is shown in Fig. 7 for composite polymer electrolyte samples containing 5, 10, and 15 wt% nanosilica from RHA and also for the filler-free sample. From Figs. 7 and 8, it is clear that the conductivity has been substantially enhanced due to the presence of the nanofiller, and out of the three filler-added samples, the maximum enhancement is obtained for the sample with 10 wt% nanosilica filler. The conductivity has increased from 9.77×10^{-6} to 1.24×10^{-4} S cm^{-1} at 30 °C due to the incorporation of the RHA

Fig. 7 Variation of ionic conductivity with inverse temperature of the polymer electrolyte samples PEO_9LiTf (*lower curve*) and $PEO_9LiTf+x$ %(wt) SiO_2(RHA) (*upper curves*) for x=5, 10, 15)

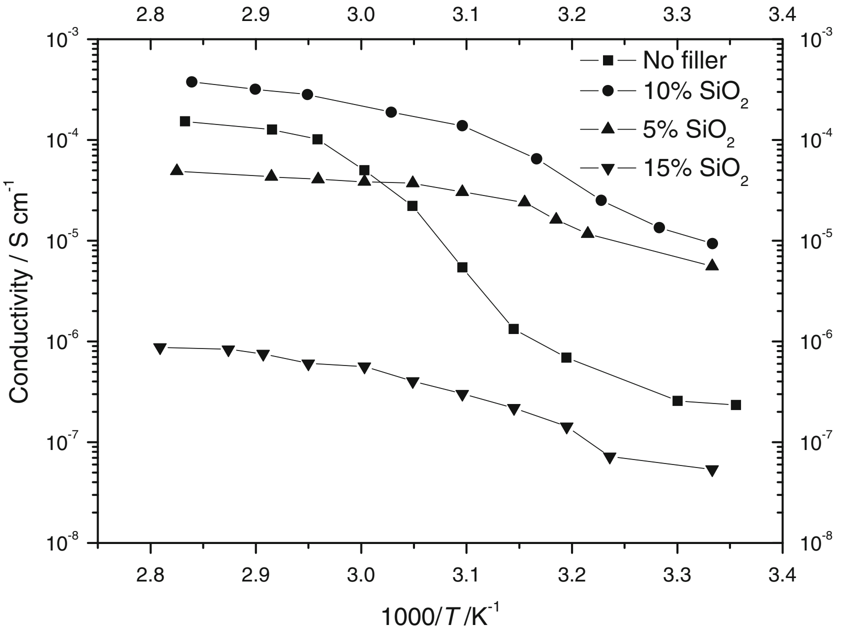

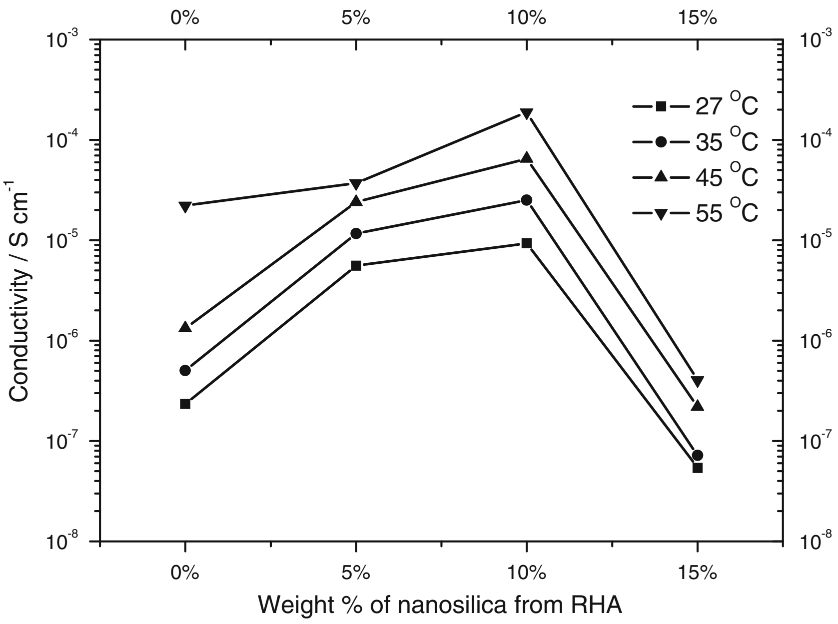

Fig. 8 Conductivity isotherms depicting the variation of conductivity with weight percent of nanosilica filler from rice husk ash in the $PEO_9LiTf+SiO_2$ composite polymer electrolyte

nanosilica filler. This is comparable to the conductivity enhancement obtained for commercial nanosilica filler for the same electrolyte under the same conditions. A comparison of ionic conductivity enhancement in PEO-based composite solid electrolytes by nanofillers taken from literature is given in Table 2.

The conductivity vs. $1/T$ plot of the filler-free sample exhibits a broad shoulder around 50–60 °C which corresponds to the crystalline-to-amorphous phase transition of the PEO electrolyte. However, this shoulder has broadened very much in the filler-added samples, suggesting that these samples already contain a larger fraction of the amorphous phase even at lower temperatures compared with the filler-free sample. The ionic conductivity enhancement can be seen also in the amorphous phase above the PEO crystallite melting temperature of about 60 °C.

Ionic conductivity enhancement due to the incorporation of nano-sized inert fillers into PEO-based polymer electrolytes has been reported by us and by several other groups earlier [3, 5]. However, all these nanofillers were commercial grade powders of alumina, titania, and silica. As already suggested by us and by others, the O^{2-} and OH^- surface groups in the filler surface interact with the Li^+ ions, and these interactions appear to provide transient hopping sites for migrating Li^+ ions through transient H bonding, creating additional high-conducting pathways [24, 25]. This would contribute to a substantial conductivity enhancement through increased ionic mobility at temperatures above as well as below the PEO crystallite melting temperature. However, an additional contribution to conductivity enhancement, particularly at temperatures below 60 °C, appears to come from the increased fraction of the amorphous phase as a result of the reduction of PEO crystallite size, as reflected from the reduced crystallite melting temperature, T_m. The essentially unchanged glass transition temperature, T_g, due to the presence of the filler suggests that the main chain dynamics of the polymer remains unchanged by the filler. This further supports that the contribution to the enhanced ionic conductivity from the polymer segmental flexibility has not changed much and that the creation of additional hopping

Table 2 Comparison of ionic conductivity enhancement with those reported by other workers

Reference	System	Conductivity, no filler (S cm^{-1})	Conductivity, with filler (S cm^{-1})	Remarks
This work	PEO_9LiTf+10 wt% SiO_2 (from RHA)	9.77×10^{-6} (30 °C)	1.24×10^{-4} (30 °C)	RHA silica, 25–40 nm
This work	PEO_9LiTf+10 wt% SiO_2 (commercial)	9.77×10^{-6} (30 °C)	1.27×10^{-4} (30 °C)	Aldrich silica, 10–20 nm
[29]	PEO_9LiTf+10 wt% SiO_2 (commercial)	10^{-7}–10^{-8} (25 °C)	2.3×10^{-5} (25 °C)	Degussa-Huls, silica filler, R805, 12 nm
[30]	$PEO_{20}LiBF_4$+15 wt% SiO_2 (commercial)	2.0×10^{-8} (25 °C)	1.1×10^{-7} (25 °C)	Aldrich silica, 10–20 nm, functionalized
[31]	PEO_9LiTf+15 wt% Al_2O_3	3.5×10^{-7} (25 °C)	2.1×10^{-5} (25 °C)	Aldrich alumina filler; pore size, 5.8 nm

sites for Li^+ ion migration as well as the increased amorphous phase content on the electrolyte material appear to be the likely mechanisms caused by the presence of the filler.

There are numerous industrial and other applications of nanosilica. For example, it has been found that by introducing nanosilica to concrete mixtures, the cracking and erosion of concrete caused by alkali silica reactivity could be minimized, resulting in long-lasting buildings, roadways, sidewalks, stairs, sewers, and dams [26]. Recent research on nanosilica-based superhydrophobic materials could eventually lead to many industrial applications. For example, a simple routine of coating cotton fabric with nanosilica particles by the sol–gel technique, which protects the fabric from UV light and makes it superhydrophobic, has been reported [27]. Similarly, silica nanoparticles can be deposited on top of already hydrophobic carbon fabric to make it superhydrophobic [21]. Using silica nanoparticles is also of interest to develop transparent hydrophobic materials for car windshields and self-cleaning windows [28]. In this paper, we have demonstrated the possibility of obtaining nanosilica from rice husk ash by a simple chemical route and established that this nanosilica essentially possesses identical structural, electrical, optical, and thermal properties to commercially available nanosilica. Ionic conductivity enhancement in PEO-based solid polymer electrolytes has been selected as one of the representative examples of many potential technological applications of this nanosilica source.

Conclusions

Pure nanosilica particles with particle size in the 30- to 45-nm range can be synthesized successfully from rice husk ash by a simple chemical route. The incorporation of these silica filler into the PEO_9LiTf polymer electrolyte has resulted in a significant enhancement in the ionic conductivity of the electrolyte.

Acknowledgments University of Peradeniya, Sri Lanka, and the International Programmes in Physical Sciences (IPPS), Uppsala University, Sweden, are gratefully acknowledged for research support.

References

1. Weston JE, Steele BCH (1982) Solid State Ionics 7:75–79
2. Gray FM (1997) In: Connor JA (ed) Polymer electrolytes. The Royal Society of Chemistry, Canterbury
3. Dissanayake MAKL, Jayathilake PARD, Bokalawela RSP, Albinson I, Mellander B-E (2003) J Power Sources 119–121:409–414
4. Bandara LRAK, Dissanayake MAKL, Mellander B-E (1998) Electrochemica Acta 43:1447–1451
5. Croce F, Persi L, Scrosati B, Serraino-Fiory F, Plichta E, Hendrickson MA (2001) Electrochemica Acta 46:2457–2461
6. Jayathilake PARD, Dissanayake MAKL, Albinson I, Mellander B-E (2002) Electrochemica Acta 47:3257–3268
7. Kelley IE, Owen JR, Steele BCH (1985) J Power Sources 14:13–21
8. Lin CW, Hung CL, Venkateswarlu M, Hwang BJ (2005) J Power Sources 146:397–401
9. Leo CJ, Subba Rao GV, Chowdari BVR (2002) Solid State Ionics 148:159–171
10. Ahn J-H, Wang GX, Liu HK, Dou SX (2003) J Power Sources 119–121:422–426
11. Kim YW, Lee W, Choi BK (2000) Electrochemica Acta 45:1473–1477
12. Thuadaij N, Nuntiya A (2008) Synthesis and characterization of nanosilica from rice husk ash prepared by precipitation method. Chiang Mai J Sci 35(1):206–211
13. Wagner C (1933) Z Physik Chem B21:25–47
14. Kyung-Ryul L, Jong-Ho L, Han-Ill Y (2010) Solid State Ionics 181:724–729
15. Shokri B, Firouzjah MA, Hosseini SI (2009). http://www.ispc-conference.org/ispcproc/papers/791.pdf
16. Waseem M, Mustafa S, Naeem A, Shah KH, Irfan S, Ihsan-ul-Haque (2009) J Pak Mater Soc 3(1):19–21
17. Xu Y-M, Q J(A), He D-M, Wang D-M, Chen H-Y, Guan J, Zhang Q-M (2010) Oil Shale 27(1):37–46. Estonian Academy Publishers
18. Haslinawati MM, Matori KA, Wahab ZA, Sidek HAA, Zainal AT (2009) Int J Basic Appl Sci IJBAS 9(9):111–117
19. Farook A, Thiam-Seng C, Jeyashelly A (2011) J Sol–Gel Sci Tech 59(3):580–583
20. Kalapathy U, Proctor A, Shultz J (2000) J Chem Technol Biotechnol 75(6):464–468
21. Chien-Te H, Fang-Lin W, Shu-Ying Y (2008) Surf Coat Technol 202(24):6103–6108
22. Suriani I, Rafie JM (2012) Int J Electrochem Sci 7:2596–2615
23. Ali AMMA, Subban RHY, Bahron H, Winnie T, Latif F, Yahya MZA (2008) Ionics 14:491–496
24. Pitawala HMJC, Dissanayake MAKL, Seneviratne VA (2007) Solid State Ionics 178:885–888
25. Wieczorek W, Lipka P, Zukowska G, Wycislik H (1998) J Phys Chem B 102:6968–6974
26. Han Y, Sukhishvili S, Du H, Cefaloni J, Smolinski B (2008) Layer-by-layer self-assembly of oppositely charged Ag nanoparticles on silica spheres as surface-enhanced Raman scattering platform. J Nanosci Nanotechnol 8:1–10
27. Chao-Hua X, Shun-Tian J, Jing Z, Li-Qiang T, Hong-Zheng C, Mang W (2008) Sci Technol Adv Mater 9(3):035008
28. Changhong S, Jun L, Hongbin G, Qingjun W, Qingmin C (2006) Appl Surf Sci 253(5):2633–2636
29. Kwang-Sun J, Hee-Soo M, Jong-Wook K, Jong-Wan P (2003) J Power Sources 117:124–130
30. Liu Y, Lee JY, Hong L (2002) J Power Sources 109:507–514
31. Piawala HMJC, Dissanayake MAKL, Seneviratne VA (2007) Solid State Ionics 178:885–888